

Novel Liquid-Crystal Phase-Transition Behavior at the Chiral Nematic-Smectic-A-Smectic-C Point

D. S. Parmar^(a) and N. A. Clark

Condensed Matter Laboratory, Department of Physics, and Center for Optoelectronic Computing Systems, University of Colorado, Boulder Colorado 80309

D. M. Walba

Department of Chemistry and Biochemistry and Center for Optoelectronic Computing Systems, University of Colorado, Boulder, Colorado 80309

M. D. Wand

Displaytech, Inc., 2200 Central Avenue, Boulder, Colorado 80301

(Received 21 December 1988)

New phenomenology of the chiral nematic (*N*), smectic-*A* (*A*), ferroelectric smectic-*C* (*C*) point (*NAC*) is reported in a binary mixture of two chiral components. We find a tricritical point on the *AC* phase-transition line which is displaced from the *NAC* point, and an *NA* line which is first order. At the *NAC* point all three transitions (*NA*, *AC*, *NC*) are first order, making it a triple point. The results suggest ways to generate a variety of additional new *NAC* behavior.

PACS numbers: 64.70.Md, 61.30.Eb

The nature of the nematic (*N*), smectic-*A* (*A*), and smectic-*C* (*C*) point in liquid-crystal binary systems has been the subject of extensive investigation over the last decade.¹⁻⁵ To date work has focused on the *NAC* phase diagram of Fig. 1(a), obtained by mixing two appropriately selected materials: component No. 1 having a

first-order *N*-to-*C* transition and component No. 2 having an *A* phase between the *N* and *C*. As the concentration of component No. 1 is increased the *A* temperature range narrows and the *NA* and *AC* lines converge, merging into the *NC* line at the *NAC* point. In systems studied the *NA* and *AC* lines exhibit second-order transitions and the *NC* line is first order, the *NC* transition entropy decreasing on approaching the *NAC* point, making it a multicritical point [Fig. 1(a)]. The recent discovery of a first-order *AC* transition⁶ and the well-known fact that the *NA* transition becomes first order when the *A* range is sufficiently narrow⁷ suggest that a variety of other *NAC* behavior is possible.

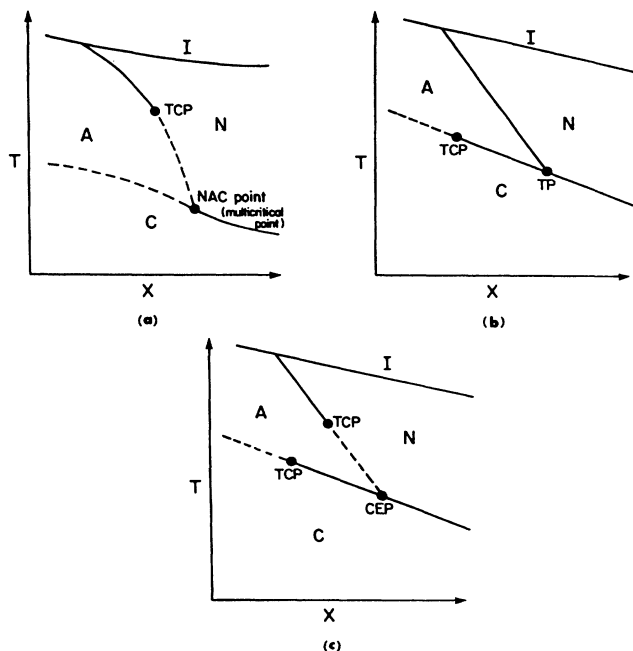


FIG. 1. (a) Typically observed *NAC* multicritical point geometry. TCP is the tricritical point. (b) *NAC* triple-point (TP) geometry reported here. (c) Geometry attainable by widening the *N* range of the $x=0$ (second-order *AC*) component. CEP is the critical end point.

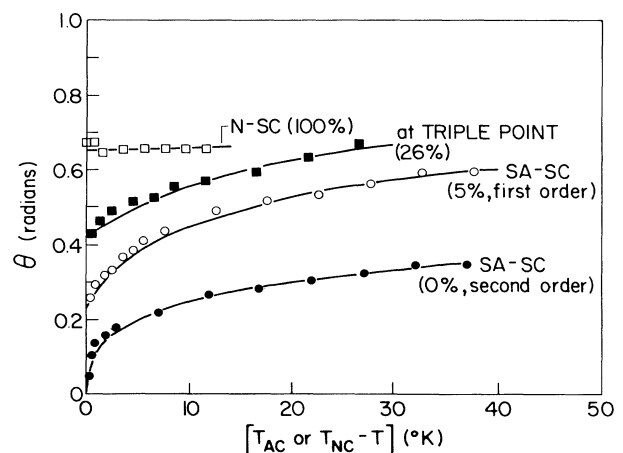


FIG. 2. Variation of tilt angle θ in the *C* phase as a function of temperature below the *AC* or the *NC* transition. Percent shown on each curve is the wt.% MDW74 in W82. The solid lines are fits by the standard mean-field model with θ^2 , θ^4 , and θ^6 terms (Ref. 4).

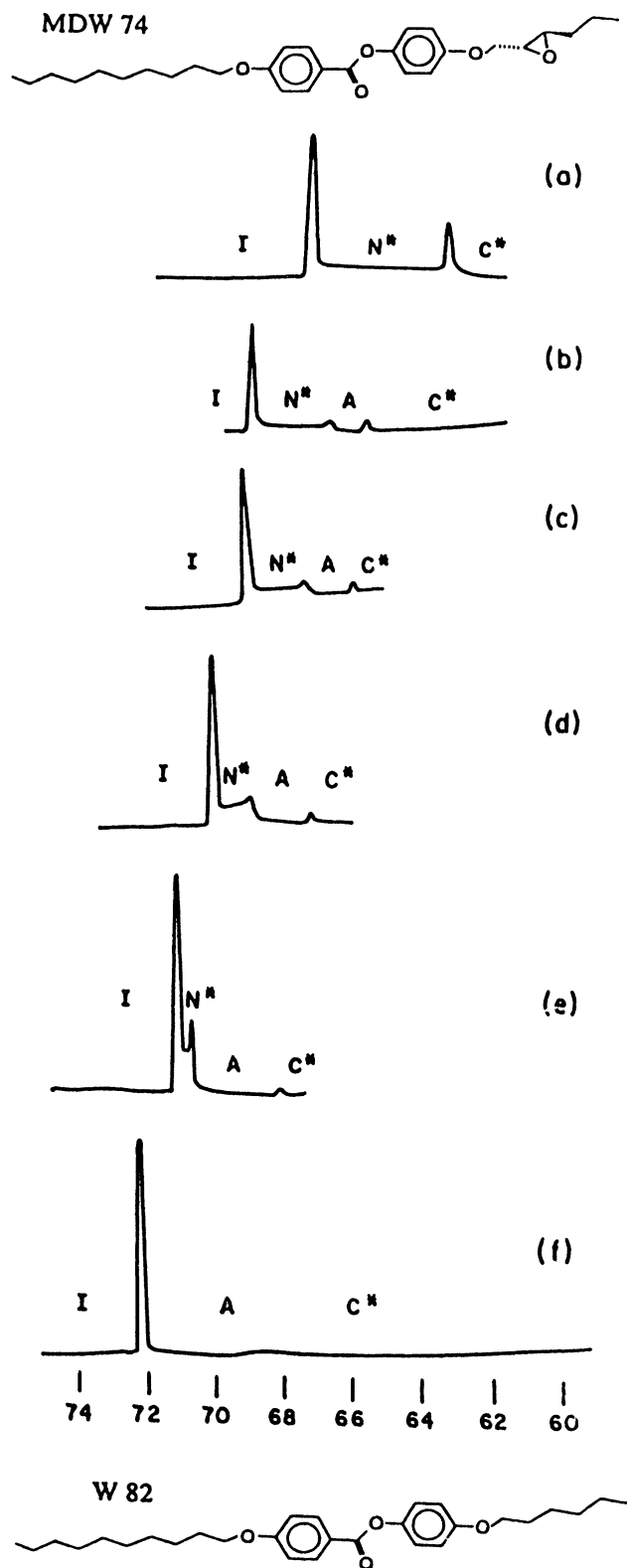


FIG. 3. Typical DTA traces at different MDW74 concentration in W82: (a) 26%, (b) 18%, (c) 15%, (d) 10%, (e) 5%, and (f) 0%.

The purpose of this Letter is to report the observation of the NAC geometry of Fig. 1(b). An AC tricritical point is observed on the AC line which makes the AC transition first order away from the NAC point. The A range is narrow enough that the NA transition is first order so that the NA , AC , and NC transitions are all first order at the NAC point, making it a triple point.

The material studied is a binary mixture of the two chiral molecules MDW74 (Ref. 8) and 1007* (W82),⁹ shown in the figures. The phase-transition temperatures and the nature of the phase transition in each mixture were determined using Mettler differential thermal analysis (DTA), optical polarized transmission microscopy, and optical determination of the director tilt angle θ in the C phases. The C phases, being ferroelectric, could be switched in director orientation by an external electric field. The temperature dependence of θ (Fig. 2) was determined for each mixture by measuring the angle between the director orientations for the opposite directions of the field. The raw DTA plots for varying weight percent of MDW74 in W82 are shown in Fig. 3. The plots were recorded on cooling the samples (~ 5 mg each) at $0.5^\circ\text{C}/\text{min}$ from the isotropic liquid phase. Similar plots with about the same phase-transition temperatures and latent heats were obtained on heating the samples from the solid phase.

The temperature-weight-percent MDW74 (W) phase diagram obtained is shown in Fig. 4. A summary of the phase-transition temperatures for each mixture is given in Table I. Our measurements of θ (Fig. 2), x-ray data on the smectic layer spacing,¹⁰ and ferroelectric polarization data¹¹ indicate that the AC transition in W82 is unambiguously second order, the typically used mean-field model with sixth-order term¹² and a positive θ^4 term fitting the data well. The N phase appears upon mixing in $\cong 2\%$ by weight of MDW74 and the A - C transition changes to first order in the same concentration range. This change is well established in the θ data at the 5% MDW74 concentration as shown in Fig. 2. The mean-field form¹² fits the θ data well with the θ^4 term changing sign at $W = (2.1 \pm 0.3)\%$. The AC heat capacity also disappears in this vicinity (Fig. 3). The AC tricritical point is at 70.7°C .

The NA line showed a heat-capacity peak of decreasing total enthalpy with increasing N range (Fig. 3). A well-defined peak remained until the intersection with the C line. It is difficult to unambiguously distinguish latent heat from enthalpy due to a heat-capacity anomaly with the limited DTA resolution, especially for the NA transition where the heat-capacity anomaly is large. Our assignment of the NA line as being first order is based on the value of the McMillan ratio, $R = T_{NA}/T_{IN} = 0.99$, at the NAC concentration. In all known nonpolar mixtures, such as those reported here, the NA transition is found to be first order for $R > 0.98$.¹³ However, the possibility of a phase diagram such as Fig. 1(c), with a tricritical point on the NA line and the NAC being a critical end point,

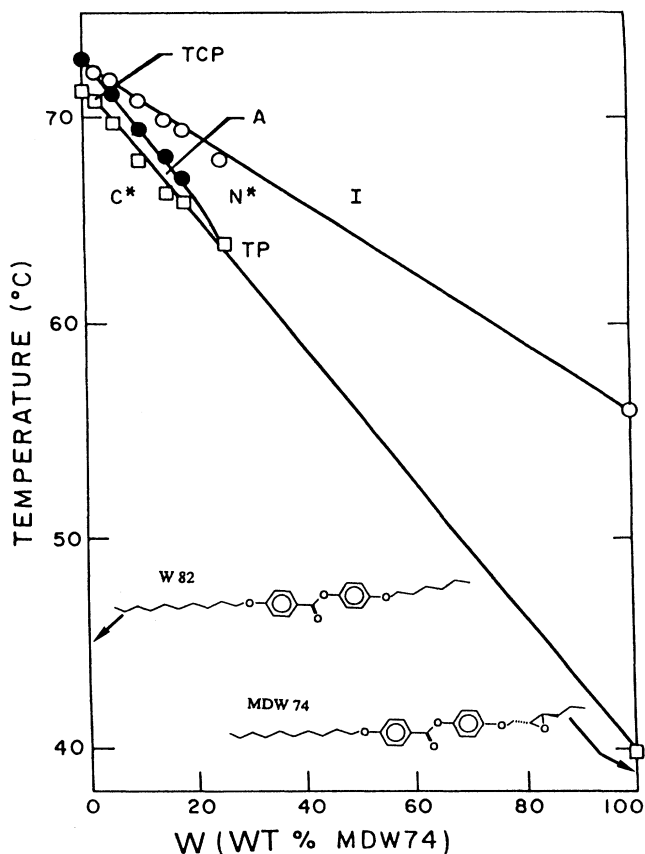
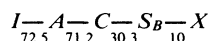
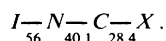


FIG. 4. Phase diagram as a function of temperature (T) and wt.% concentration of MDW74 in W82 (W). W82 has a phase sequence of



and MDW74 has the phase sequence of



TCP is the tricritical point on the AC line and the TP is the NAC triple point.

cannot be entirely ruled out with the data at hand. An NAC critical end point would make the AC line continuous through the NAC point. The data show at most a weak break, suggesting that the NA transition is weakly first order compared to the NC . The NC line is strongly first order along its entire length.

The data show several other features of interest. Defining the "saturation" tilt angle θ_{sat} to be that at $(T_{NC} \text{ or } T_{AC}) - T = 35 \text{ K}$, Fig. 2 shows that θ_{sat} increases remarkably rapidly with MDW74 concentration from the W82 value of $\theta_{\text{sat}} = 18^\circ$ to near $\theta_{\text{sat}} = 38^\circ$, the MDW74 value at only 5% MDW74. This indicates that the energy maintaining MDW74 tilt is large compared to that of W82 and we believe that it is this difference that produces the AC tricritical behavior in our mixture.

TABLE I. Phase-transition temperatures for MDW74 and W82 mixtures.

MDW74 (%)	T_{IN} ($^\circ\text{C}$)	T_{NA} ($^\circ\text{C}$)	T_{AC} ($^\circ\text{C}$)
0			71.2
2	71.8	71.4	68.8
5	71.6	71	68.7
10	70.0	69.4	67.6
15	69.8	67.9	66.5
18	69.2	67.7	67.2
26	67.7	63.7	63.7

Clearly MDW74 has a strong coupling of the layering and tilt order parameters which, even at extreme dilution, is sufficient to drive the AC transition first order. Thus we would expect a significant jump in the layer order parameter (i.e., stronger and higher-order Bragg cusps) in the C phase where the AC transition is first order. We would further expect the chiral nature of the transitions to be unrelated to the appearance of a first-order AC transition in this mixture, in contrast to a recent report on a different mixture.¹⁴

Figure 4 suggests several interesting variations of the mixture components. Choosing the second-order AC material to have a larger N range will almost certainly cause the phase diagram to evolve in the direction of that in Fig. 1(c). Varying the N range with two-component second-order material or by selecting homologs may allow the continuing variation of the NA TCP location on the NA line and enable study of a $TP \rightarrow CEP + TCP$ evolution. Similar movement of the TCP on the AC line should also be possible although the guidelines for selection of the second-order material are less obvious in this case.

This work was supported by U.S. ARO Grant No. DAAL-03-86-K-0053 and NSF Grant No. CDR-8622236 through the National Science Foundation Engineering Research Center for Optoelectronic Computing Systems.

^(a)Permanent address: Department of Physics, University of Kashmir, Srinagar 190006, India.

¹D. L. Johnson, D. Allender, R. DeHoff, C. Maze, E. Oppenheim, and R. Reynolds, Phys. Rev. B **16**, 470 (1977).

²R. DeHoff, R. Biggers, D. Brisbin, and D. L. Johnson, Phys. Rev. A **25**, 472 (1982).

³C. R. Safinya, R. J. Birgeneau, J. D. Litster, and M. L. Neubert, Phys. Rev. Lett. **47**, 668 (1981).

⁴C. C. Huang and S. C. Lien, Phys. Rev. Lett. **35**, 1678 (1975).

⁵L. J. Martinez-Miranda, A. R. Kortan, and R. J. Birgeneau, Phys. Rev. A **36**, 2372 (1987).

⁶B. R. Ratna, R. Shashidhar, Geetha G. Nair, S. Krishna Prasad, Ch. Bahr, and G. Heppke, Phys. Rev. A **37**, 1824

(1988).

⁷W. L. McMillan, Phys. Rev. A **6**, 936 (1972).

⁸MDW74 is 4-[(2*R*,3*R*)-epoxyhexyloxy]phenyl-4-[(3*S*,7)-dimethyloctyloxy]benzoate obtained from Displaytech, Inc., Boulder, CO 80301.

⁹W82 is 4'[(*s*)-(4-methylhexyl)oxy]phenyl 4-(decyloxy)-benzoate described in P. Keller, Ferroelectrics **58**, 3 (1984), obtained from Displaytech, Inc., Boulder, CO 80301.

¹⁰P. Keller, P. E. Cladis, P. L. Finn, and H. R. Brand, J. Phys. (Paris) **46**, 2203 (1985).

¹¹D. S. Parmer and N. A. Clark (to be published).

¹²C. C. Huang and J. M. Viner, Phys. Rev. A **25**, 3385 (1982).

¹³M. E. Huster, K. J. Stine, and C. W. Garland, Phys. Rev. A **36**, 2364 (1987).

¹⁴J. Huang and J. T. Ho, Phys. Rev. Lett. **58**, 2239 (1987).